Article

Discovery Medicine 2026; 38(214): 3522–3541
https://doi.org/10.24976/Discov.Med.202638214.269

LFNG Is Downregulated in Preeclamptic Placenta and Promotes Trophoblast Proliferation and Invasion and Suppresses NOTCH4 Upregulation Under Chemically Induced Hypoxia

Qi Peng[1,2,†], Wenjing Zhang[1,†], Lanling Fan[2], Yongguo Yang[3], Su Wan[4], Chenggan Shu[5], Weipei Zhu[1,*]

[1]Department of Obstetrics and Gynecology, The Second Affiliated Hospital of Soochow University, 215000 Suzhou, Jiangsu, China
[2]Department of Obstetrics and Gynecology, Jiangdu People's Hospital Affiliated to Yangzhou University, 225200 Yangzhou, Jiangsu, China
[3]Department of Pathology, Jiangdu People's Hospital Affiliated to Yangzhou University, 225200 Yangzhou, Jiangsu, China
[4]Department of Gynecology, The First Affiliated Hospital of Wannan Medical University, 241000 Wuhu, Anhui, China
[5]Department of Obstetrics and Gynecology, Yancheng First Hospital, Affiliated Hospital of Nanjing University Medical School, 224001 Yancheng, Jiangsu, China
*Correspondence: zwp333xx@126.com (Weipei Zhu)
[†]These authors contributed equally.
Submitted: 25 August 2026 Revised: 9 September 2026 Accepted: 8 October 2026 Published: 25 November 2026

Background: Preeclampsia affects 2–8% of pregnancies and is associated with impaired trophoblast proliferation and invasion, yet delivery of the placenta remains the only definitive treatment. NOTCH receptor responsiveness is modulated by fringe glycosyltransferases; however, whether lunatic fringe (LFNG) functions in the human placenta and whether its expression is altered in preeclampsia remain unclear.

Methods: Search Tool for the Retrieval of Interacting Genes/Proteins (STRING) was used to assess the relationship between LFNG and the NOTCH receptors. LFNG and NOTCH4 were measured in placentas from 20 women with preeclampsia and 20 normotensive women. LFNG was overexpressed in HTR-8/SVneo and JAR cells, and proliferation, invasion, subcellular localization, and NOTCH4 abundance were assessed under normoxia and $CoCl_2$-induced chemical hypoxia in a 2 × 2 factorial design. In a preventive experimental design, an Lfng-expressing adenovirus was delivered on gestational day 8.5, three days before the induction of a preeclampsia-like phenotype by Nω-nitro-L-arginine methyl ester (L-NAME) in pregnant mice.

Results: In preeclamptic placenta, the LFNG-positive area fell from a median of 5.68% (interquartile range [IQR] 5.26–6.06) to 0.03% (IQR 0.01–0.06) and *LFNG* mRNA fell to 27% of the control level, whereas *NOTCH4* mRNA rose approximately 9.5-fold. LFNG overexpression enhanced proliferation, colony formation, and Matrigel invasion in both cell lines, and LFNG shared a Golgi-associated perinuclear distribution with NOTCH4. The effect of LFNG on NOTCH4 differed between standard culture and a $CoCl_2$-induced hypoxia-like state (interaction $p < 0.0001$). NOTCH4 increased under standard culture, whereas the $CoCl_2$-driven induction was attenuated, with hypoxia-inducible factor 1-alpha (HIF-1α) stabilization unaffected. In mice, systemically delivered Lfng-expressing adenovirus (Ad-Lfng) given before L-NAME attenuated the development of the phenotype, with lower blood pressure, more live fetuses, less placental and renal injury and normalized placental Notch4, although protection was only partial.

Conclusions: LFNG is markedly reduced in preeclamptic placentas, promotes trophoblast proliferation and invasion, and restrains NOTCH4 induction in a $CoCl_2$-induced hypoxia-like state, identifying the LFNG-NOTCH4 relationship as a candidate axis in preeclampsia whose causal role remains to be established.

Keywords: preeclampsia; LFNG; NOTCH4; trophoblast; fringe glycosyltransferase; chemical hypoxia

Introduction

Preeclampsia affects approximately 2–8% of pregnancies worldwide and remains a leading cause of maternal and perinatal morbidity and mortality [1]. Despite decades of investigation, clinical management has changed little. Antihypertensive therapy can control severe hypertension and magnesium sulfate reduces the risk of eclampsia [2], but the only definitive treatment remains delivery of the fetus and dysfunctional placenta, which may be required before fetal maturity [3]. Consequently, preeclampsia is among the leading indications for iatrogenic preterm birth [4]. The absence of a disease-modifying therapy reflects an incomplete understanding of the molecular events that initiate the

Copyright: © 2026 The Author(s). Published by Discovery Medicine. This is an open access article under the CC BY 4.0 license.
Note: *Discovery Medicine* stays neutral with regard to jurisdictional claims in published maps and institutional affiliations.

disorder [5,6]. New therapeutic targets are therefore most likely to be found among these early molecular events [7].

The prevailing model locates the origin of preeclampsia in the first half of pregnancy [8]. In this two-stage framework, deficient placentation in early gestation is followed by the maternal syndrome of the second half [9], a sequence shared with other great obstetrical syndromes [10]. Proliferative trophoblast progenitors within the anchoring villous cell columns differentiate into extravillous trophoblasts [11], which invade the decidua and maternal spiral arteries and contribute to their transformation from narrow, muscular, high-resistance vessels into dilated, low-resistance conduits [12]. When invasion is shallow and remodeling is incomplete, placental perfusion becomes intermittent and inadequate, villous tissue is exposed to ischemia and oxidative stress [13,14], and antiangiogenic factors are released into the maternal circulation, producing endothelial dysfunction that manifests as hypertension and end-organ injury [15]. Trophoblast proliferation and invasion are therefore central to the development of preeclampsia, making the pathways that govern these behaviors of particular interest.

Notch signaling is one such pathway [16]. In mammals, four NOTCH receptors (NOTCH1-4) signal through the canonical cell-surface ligands JAG1, JAG2, DLL1, DLL3 and DLL4, generally requiring direct contact between adjacent cells [17]. Ligand engagement induces ADAM-mediated S2 cleavage followed by γ-secretase-mediated S3 cleavage, releasing the Notch intracellular domain (NICD), which translocates to the nucleus, associates with RBPJ/CSL and MAML coactivators, and induces a context-dependent transcriptional program that commonly includes HES and HEY family genes and NRARP [17]. In the placenta, Notch signaling controls trophoblast stem-cell expansion and differentiation [16] and has been linked to extravillous trophoblast migration and endovascular invasion [18]. Pathway disturbances have been documented in early-onset preeclamptic tissue, involving both the HEY1 branch of the pathway [19] and the Notch-associated factor EGFL7 [20]. Among the four receptors, NOTCH4 is most closely associated with the vascular endothelium [21]. Single-cell and spatial profiling of the human placenta further indicates that NOTCH receptor expression varies among trophoblast subtypes and across gestation [22]. NOTCH4 is therefore particularly relevant to the vascular compartment implicated in the development of preeclampsia.

What has received far less attention is the machinery that determines how a Notch receptor responds to its ligands. Receptor sensitivity is not fixed. POFUT1 adds O-fucose to consensus sites within folded EGF-like repeats of the Notch ectodomain, after which the mammalian fringe β-1,3-N-acetylglucosaminyltransferases LFNG, MFNG, and RFNG extend selected O-fucose glycans with N-acetylglucosamine [17], thereby altering ligand selectivity and, in many receptor-ligand contexts, enhancing Delta-like signaling while attenuating Jagged-mediated activation [23]. Fringe enzymes thus act as modulators rather than switches, adjusting pathway activity without simply turning it on or off. LFNG was initially studied as an oscillatory modulator of Notch signaling during vertebrate somitogenesis [24] and has subsequently been implicated, in a context-dependent manner, in Notch regulation and tumor biology across multiple malignancies [25,26], but whether it functions in the human placenta and whether its expression is altered in preeclampsia have not, to our knowledge, been addressed.

Further, preeclamptic placentas, particularly in early-onset disease associated with placental dysfunction, are characterized by impaired and often fluctuating oxygenation rather than uniformly sustained hypoxia [27]. By contrast, many trophoblast cell-line experiments are conducted under atmospheric oxygen (~21% O_2), a supraphysiological condition relative to the low-oxygen environment of the placental intervillous space [27,28]. Because oxygen tension can alter Notch pathway activity [29], the effects of a fringe enzyme measured under standard atmospheric-oxygen culture conditions may not accurately predict its behavior in the abnormal oxygen environment of the preeclamptic placenta [27]. We therefore included a chemically induced hypoxia-like state as an experimental variable rather than performing all experiments under standard culture conditions alone.

Guided by database-predicted interactions between LFNG and the Notch receptors, we investigated the LFNG-NOTCH4 relationship along three converging lines. LFNG and NOTCH4 were measured in paired clinical specimens. LFNG was overexpressed in two trophoblast lines to assess its effects on proliferation and invasion, its subcellular relationship with NOTCH4, and its influence on NOTCH4 under normoxia and chemically induced hypoxia in a two-factor design. Lfng was then delivered in a mouse model of preeclampsia-like hypertension to determine whether the reciprocal relationship between Lfng and Notch4 is recapitulated *in vivo*. The results identify LFNG as a placental factor reduced in preeclampsia and as a positive regulator of trophoblast proliferation and invasion, and show that its effect on NOTCH4 reverses direction when cells are exposed to a $CoCl_2$-induced hypoxia-like state.

Methods

Protein-Protein Interaction Network Analysis

Interaction relationships among the fringe glycosyltransferases, the four NOTCH receptors, and selected pathway members were retrieved from Search Tool for the Retrieval of Interacting Genes/Proteins (STRING) v12.0 (https://string-db.org/) with the organism restricted to Homo sapiens and the minimum required interaction score set to 0.700. Networks were exported directly from the STRING

interface, and the combined confidence scores are given in the legend to Fig. 1.

Study Population and Clinical Specimens

This was a prospective case-control study conducted at the Department of Obstetrics and Gynecology, Jiangdu People's Hospital Affiliated to Yangzhou University. Ethical approval was granted on 21 January 2022, and recruitment began thereafter. The first participant was enrolled and provided consent on 1 February 2022, and the last placenta was collected on 31 January 2023. All recruitment, informed consent, and sample collection therefore took place after the date of ethical approval, and no previously stored or archived clinical specimens were used. Placental tissue was obtained from 20 women with preeclampsia and 20 normotensive women with uncomplicated pregnancies.

Preeclampsia was diagnosed by two independent obstetricians according to the criteria of the American College of Obstetricians and Gynecologists [30]: New-onset systolic blood pressure ≥140 mmHg and/or diastolic blood pressure ≥90 mmHg on at least two occasions at least 4 h apart after 20 weeks of gestation in a previously normotensive woman, accompanied by proteinuria (≥300 mg per 24 h urine collection, a protein/creatinine ratio ≥0.3, or a dipstick reading of 2+ when quantitative methods were unavailable). In the absence of proteinuria, the diagnosis required new-onset thrombocytopenia (platelet count <100 $\times 10^9$/L), renal insufficiency (serum creatinine >1.1 mg/dL or a doubling of the baseline value), impaired liver function (transaminase levels at least twice the upper limit of normal), pulmonary edema, or new-onset cerebral or visual symptoms.

Inclusion criteria for both groups were singleton pregnancy, spontaneous conception, maternal age of 20–40 years, and gestational age confirmed by the last menstrual period and first-trimester ultrasound. Exclusion criteria were chronic hypertension or other pre-existing hypertensive disorders, pre-gestational or gestational diabetes, chronic renal disease, autoimmune or thyroid disease, intrahepatic cholestasis of pregnancy, clinical or histological chorioamnionitis or other intrauterine infection, premature rupture of membranes, placental abruption or placenta previa, fetal chromosomal or structural anomalies, multiple gestation, assisted reproductive technology, and maternal smoking or alcohol use during pregnancy.

Control subjects were normotensive women (blood pressure <140/90 mmHg throughout gestation, no proteinuria and no other hypertensive complications) with otherwise uncomplicated pregnancies, recruited over the same period at the same institution and satisfying the same inclusion and exclusion criteria. To eliminate the transcriptional effects of labor, placentas in both groups were collected from elective caesarean deliveries performed before the onset of labor. In the control group, the indications were previous caesarean section, breech presentation, or maternal request. Because of the restrictive exclusion criteria and the requirement for delivery by elective caesarean section before the onset of labor, twenty case-control pairs meeting all criteria were available over this period. These criteria also excluded premature rupture of membranes, placental abruption, and other indications for early delivery; consequently, all deliveries in both groups occurred at term, and no woman in either group delivered preterm. Gestational age at delivery was nevertheless slightly lower in the preeclamptic group, although the two distributions overlapped substantially. Recruiting normotensive controls who delivered earlier would have required the presence of another pregnancy complication and would have replaced one source of imbalance with another. The clinical characteristics of both groups are summarized in Table 1. Written informed consent was obtained from every participant before delivery.

Placental Sampling and Tissue Processing

Placentas were collected immediately after delivery and processed within 1 hour. Sampling followed a standardized protocol applied identically to both groups. Four full-thickness villous tissue blocks of approximately 1 cm^3 were excised from the maternal side of the placenta, midway between the cord insertion and the placental margin, with one block taken from each quadrant. The outer 2 cm of the placental rim was avoided, as were any macroscopically visible areas of infarction, calcification, hemorrhage or thrombosis. Tissue blocks were rinsed repeatedly in ice cold sterile phosphate buffered saline until the effluent was free of maternal blood. Each specimen was then divided. One portion was snap-frozen within 30 min of delivery and stored at –80 °C for RNA and protein extraction, and the remaining portion was immersion-fixed in 4% paraformaldehyde at room temperature for 24 h before dehydration and paraffin embedding. All specimens were collected by the same two operators throughout the study.

Immunohistochemistry

Fixed tissue was processed through graded ethanol, cleared in xylene, embedded in paraffin, and cut into 4 µm sections. Sections were dewaxed, rehydrated, and subjected to heat-induced epitope retrieval in citrate buffer at pH 6.0 (G1202, Servicebio, Wuhan, China). Endogenous peroxidase was quenched with 3% hydrogen peroxide (10 min, room temperature) and non-specific binding was blocked with 3% goat serum for 30 min. Primary antibodies were applied overnight at 4 °C at the following dilutions: rabbit polyclonal anti-LFNG (HPA069130, Atlas Antibodies, Bromma, Sweden, 1:200), rabbit polyclonal anti-CD31 (28083-1-AP, Proteintech, Wuhan, China, 1:200), rabbit polyclonal anti-CK7 (15539-1-AP, Proteintech, Wuhan, China, 1:200) and mouse monoclonal anti-HLA-G (MA1-19219, Invitrogen, Waltham, MA, USA, 1:200). After washing, sections stained for LFNG, CD31

Table 1. Clinical characteristics of the study population.

Variable	Preeclampsia (n = 20)	Normotensive control (n = 20)	*t*	*p*
Maternal and obstetric characteristics				
Gravidity	1 (1, 2)	2 (1, 3)	-	-
Parity	0 (0, 1)	0 (0, 1)	-	-
Gestational age at delivery (weeks)	38.64 (38.00, 39.40)	39.14 (38.71, 39.57)	-	-
Hemodynamic measurements				
Systolic blood pressure (mmHg)	144.25 ± 13.64	118.26 ± 10.04	6.863	<0.0001
Diastolic blood pressure (mmHg)	87.23 ± 9.49	74.39 ± 7.68	4.704	<0.0001
Pulse (beats/min)	88 (84, 90)	88 (80, 92)	-	-
Laboratory findings				
Platelet count ($\times 10^9$/L)	153.9 ± 36.5	145.6 ± 32.1	0.764	0.450
Mean corpuscular hemoglobin concentration (g/L)	328.45 ± 10.52	330.09 ± 11.11	–0.479	0.634
Globulin (g/L)	26.17 ± 3.53	26.64 ± 3.54	–0.420	0.677
Uric acid (μmol/L)	336.17 ± 72.99	316.25 ± 70.06	0.881	0.384
Potassium (mmol/L)	4.17 (3.86, 4.38)	4.03 (3.91, 4.20)	-	-
Thrombin time (s)	15.70 (15.23, 16.38)	15.70 (15.13, 16.18)	-	-
Urine specific gravity	1.020 ± 0.008	1.019 ± 0.007	0.421	0.676
Neonatal outcome				
Birth weight (kg)	3.30 (2.88, 3.59)	3.50 (3.20, 3.62)	-	-

Data are presented as mean ± SD or median (interquartile range) according to distribution. Normally distributed variables were compared by unpaired two-tailed Student's *t* test, with *t* calculated as preeclampsia minus normotensive control. Non-normally distributed variables are presented descriptively. Both groups met identical inclusion and exclusion criteria. Maternal age was restricted to 20–40 years, and all pregnancies were singleton and spontaneously conceived. All deliveries in both groups were by elective caesarean section performed before the onset of labor, and all occurred at term (≥37 weeks). No woman in either group delivered preterm. Preeclampsia was diagnosed in 20 of 20 women in the preeclampsia group and in none of the control group, according to the criteria detailed in Methods. SD, standard deviation.

and CK7 were incubated with an horseradish peroxidase (HRP)-conjugated goat anti-rabbit IgG secondary antibody (GB23303, Servicebio, Wuhan, China, 1:1000), whereas sections stained for HLA-G were incubated with an HRP-conjugated goat anti-mouse IgG secondary antibody (GB23301, Servicebio, Wuhan, China, 1:1000), for 50 min at 37 °C. Both secondary antibodies were raised in goats and were therefore compatible with the goat serum used for blocking. Sections were developed with diaminobenzidine under microscopic control, counterstained with hematoxylin, dehydrated and mounted. Negative controls were processed in parallel, with the primary antibody replaced by PBS.

Slides were imaged using a light microscope (E100, Nikon Corporation, Tokyo, Japan). For quantification, 3 non-overlapping fields per case were captured under identical illumination and exposure settings by an operator blinded to group assignment. Positive signal was separated from the hematoxylin counterstain by color deconvolution in ImageJ (version 1.54b, National Institutes of Health, Bethesda, MD, USA), and the LFNG-positive fraction was expressed as the percentage of the total tissue area occupied by 3,3'-diaminobenzidine (DAB)-positive pixels, using a threshold held constant across all images. Values from the three fields for each case were averaged to yield a single value per specimen.

Cell Culture and Gene Transfer

HTR-8/SVneo human extravillous trophoblast cells and JAR human choriocarcinoma cells were obtained from the cell bank of the Chinese Academy of Sciences (Shanghai, China) and grown at 37 °C under 5% CO_2 in Roswell Park Memorial Institute (RPMI)-1640 supplemented with 10% fetal bovine serum and penicillin-streptomycin. Cultures were passaged at 80–90% confluence. The cell lines were authenticated by Short Tandem Repeat profiling, and mycoplasma testing was negative throughout.

The LFNG overexpression construct was prepared by GenePharma (Shanghai, China). The full-length human *LFNG* coding sequence (NM_001040167.2, encoding 379 amino acids) was cloned into the pcDNA3.1(+) backbone (V79020, Invitrogen, Carlsbad, CA, USA) between the *Hin*dIII and *Xho*I sites, immediately downstream of the CMV promoter, to generate the overexpression construct (OE-LFNG). No epitope tag was appended to the coding sequence. The empty pcDNA3.1(+) vector, identical to the backbone of OE-LFNG but carrying no insert, was supplied by the same manufacturer (GenePharma, Shanghai, China) and served as the negative control (OE-NC). Both plasmids were prepared in parallel from the same vector stock, propagated in *Escherichia coli* DH5α, and purified with an endotoxin-free plasmid kit. The identity, orientation and reading frame of the insert were verified by restric-

tion digestion and bidirectional Sanger sequencing across the entire insert and both vector-insert junctions, and the sequence was identical to the reference. Cells were seeded the day before transfection to reach approximately 70% confluence, and 2.5 µg of plasmid was introduced per well using Lipofectamine 3000 (L3000015, Invitrogen, Waltham, MA, USA) in serum-free medium. Identical amounts of OE-NC and OE-LFNG plasmid were used, and the total mass of DNA per well was the same in all conditions. The transfection mixture was replaced with complete medium after 6 h, and cells were harvested 48 h after transfection for validation and all downstream assays. Chemical hypoxia was induced by adding cobalt chloride to a final concentration of 150 µM for 24 h. Control cultures received an equal volume of vehicle. Four conditions were compared in a 2 × 2 factorial arrangement: OE-NC, OE-LFNG, OE-NC with $CoCl_2$, and OE-LFNG with $CoCl_2$.

Quantitative Real-Time Polymerase Chain Reaction (PCR)

Total RNA was recovered from tissue or cell pellets in TRIzol Universal Reagent (DP424, TIANGEN, Beijing, China), and its concentration and purity were checked spectrophotometrically. Only preparations with an A260/A280 ratio between 1.8 and 2.1 were carried forward. Reverse transcription of 1000 ng of RNA was performed with a Vazyme kit (Cat. RT101-01, Vazyme, Nanjing, China) under the cycling conditions specified for the kit. Amplification was carried out on a LightCycler96 instrument (Roche, Mannheim, Germany) in 20 µL reactions containing SYBR qPCR master mix (Cat. Q312-02, Vazyme, Nanjing, China). Melt-curve analysis at the end of each run confirmed a single amplicon. Glyceraldehyde-3-phosphate dehydrogenase (*GAPDH*) served as the internal reference, and relative abundance was derived using the $2^{-\Delta\Delta Ct}$ method. Because GAPDH is a glycolytic enzyme and a recognized HIF-1 target, its suitability as a normalizer under chemical hypoxia was examined directly. Raw Cq values for *GAPDH* were compared across the four experimental conditions by one-way analysis of variance with Tukey's post-hoc test, and the resulting confidence intervals were converted to fold-differences in transcript abundance. In addition, because reverse transcription was performed using a fixed input of 1000 ng of total RNA of verified purity, raw *NOTCH4* Cq values, which are independent of any reference gene, were analyzed in parallel by two-way analysis of variance. Every sample was assayed in triplicate wells, and the mean of the three wells was treated as one biological observation. Primer sequences are listed in Table 2.

Western Blotting

Cells and pulverized placental tissue were lysed in radioimmunoprecipitation assay (RIPA) buffer (P0013J, Beyotime, Shanghai, China) containing protease and phosphatase inhibitors (ST506, Beyotime, Shanghai, China), kept on ice for 30 min with intermittent vortexing, and clarified at 12,000 ×g for 15 min at 4 °C. Protein concentration was determined by bicinchoninic acid (BCA) assay. Equal protein loads of 20–30 µg were resolved on 10% sodium dodecyl sulfate-polyacrylamide gel electrophoresis (SDS-PAGE) gels (P0015, Beyotime, Shanghai, China) and transferred to polyvinylidene fluoride (PVDF) membranes (IPVH00010, Millipore, Burlington, MA, USA) for 40 min. Membranes were blocked in 5% non-fat milk in Tris-buffered saline containing Tween 20 (TBST) for 1 h at room temperature and probed overnight at 4 °C with antibodies against LFNG (ab151699, abcam, 1:1000), NOTCH4 (33280-1-AP, Proteintech, Wuhan, China, 1:1000), HIF-1α (20960-1-AP, Proteintech, Wuhan, China, 1:1000) or GAPDH (60004-1-Ig, Proteintech, Wuhan, China, 1:1000). After three TBST washes, an HRP-conjugated secondary antibody (ZB-2301/2305, ZS Golden Bridge, Beijing, China, 1:2000) was applied for 1 h at room temperature. Signal was developed with enhanced chemiluminescence substrate (WBKLS0500, Millipore, Burlington, MA, USA). For NOTCH4, the band at approximately 210 kDa, corresponding to the full-length receptor, was quantified; the cleaved intracellular fragment was not quantified. Band intensities were measured using ImageJ software (version 1.54b, National Institutes of Health, Bethesda, MD, USA), normalized to the GAPDH signal in the same lane, and expressed relative to the control group of that blot. Because equal quantities of total protein, determined by BCA assay, were loaded in every lane, the stability of GAPDH itself was assessed in the $CoCl_2$ experiment. The integrated GAPDH band density of each lane was expressed relative to the mean band density of the four lanes on the same membrane, and the four experimental conditions were compared by one-way analysis of variance with Tukey's post-hoc test.

Proliferation Assays

For the cell counting kit-8 (CCK-8) assay, transfected cells were plated at 3000 cells per well in 96-well plates. At 24, 48, 72 and 96 h, 10 µL of CCK-8 reagent (A311-01, vazyme, China) was added to each well, and the plates were returned to the incubator for a further 2 h before absorbance at 450 nm was measured using a microplate reader. Wells containing medium and reagent but no cells served as blanks.

For colony formation, 500 cells were seeded per well in six-well plates and left undisturbed for 14 days, with the medium exchanged every three days. Colonies were then fixed in 4% paraformaldehyde for 15 min, stained with 0.1% crystal violet (G1064, Solarbio, Beijing, China) for 20 min, rinsed and air-dried. Aggregates containing more than 50 cells were scored as colonies and counted in Fiji by an observer blinded to treatment.

Table 2. Primer sequences.

Gene	Forward (5′-3′)	Reverse (5′-3′)
Human-*LFNG*	GTCAAGACCACCAAAAAGTTCCA	AGCCATGGCCACTAGAAGATG
Human-*NOTCH4*	AAGATGCCCAGGACAACAGG	ACGTGGAAGATGTCTGCTCTG
Human-*GAPDH*	TTTTGCGTCGCCAGCC	ATGGAATTTGCCATGGGTGGA
Mouse-*Lfng*	AGGACACTTCATGAGCACGG	CTGCTACAATCAGCACCCAC
Mouse-*Notch4*	TCAAGTTGCCTGGGGTCTTC	GCACTTTTTCCATCTCACCCTT
Mouse-*Gapdh*	GCATCTTCTTGTGCAGTGCC	TGAAGTCGCAGGAGACAACC

Transwell Invasion Assay

Matrigel (Cat. 356234, Corning) was thawed on ice, diluted 1:9 in serum-free medium, and used to coat the upper surface of 8 µm polycarbonate inserts (TCS-003-024, BIOFIL, Guangzhou, China), which were then allowed to gel for 0.5 h at 37 °C. Transfected cells suspended in serum-free medium (5×10^4 cells in 200 µL) were added to the upper chamber, while the lower chamber received 600 µL of medium containing 10% fetal bovine serum as a chemoattractant. After 24 h, cells remaining on the upper surface of the membrane were removed with a cotton swab, and those that had traversed the membrane were fixed in 4% paraformaldehyde and stained with 0.1% crystal violet. Five randomly selected fields per insert were photographed, and the mean count across these fields was taken as the value for that insert.

Immunofluorescence

HTR-8/SVneo cells were seeded onto 12-mm glass coverslips in 24-well plates and grown to approximately 60% confluence. Coverslips were rinsed twice in PBS, fixed in 4% paraformaldehyde (P0099, Beyotime, Shanghai, China) for 20 min at room temperature, washed three times for 5 min in PBS, permeabilized with 0.3% Triton X-100 (T8200, Solarbio, Beijing, China) for 15 min, and washed again. Non-specific binding was blocked with 5% normal donkey serum in PBS for 1 h at 37 °C.

Coverslips were then incubated overnight at 4 °C with a cocktail of three primary antibodies raised in three different host species so that each antigen could be detected by a species-specific secondary reagent. The primary antibodies included rabbit anti-LFNG (HA721367, clone JE66-62, HUABIO, Hangzhou, China; 1:100), goat anti-NOTCH4 (AF3847, R&D Systems, Minneapolis, MN, USA; 15 µg/mL) and mouse anti-GM130 (66662-1-Ig, clone 2A4F11, Proteintech, Wuhan, China; 1:800). After three 5-min washes in PBS, coverslips were incubated for 1 h at room temperature in the dark with a cocktail of highly cross-adsorbed donkey secondary antibodies, all raised in the same host species and pre-adsorbed against the other species used (Invitrogen, Thermo Fisher Scientific, Waltham, MA, USA; each 1:500), including Alexa Fluor 647 donkey anti-rabbit IgG (H+L) (A-31573) for LFNG, Alexa Fluor 555 donkey anti-goat IgG (H+L) (A-21432) for NOTCH4 and Alexa Fluor 488 donkey anti-mouse IgG (H+L) (A-21202) for GM130. Nuclei were counterstained with DAPI (C0060, Solarbio) for 10 min in the dark. Coverslips were washed, mounted in anti-fade medium (S2100, Solarbio) and sealed.

Images were acquired with an LG-FS80 digital slide scanner (Servicebio, Wuhan, China). The DAPI (excitation 377/50 nm, emission 447/60 nm), SpGreen (494/20, 527/20), SpOrange (543/22, 586/20) and Cy5 (628/40, 692/40) channels were captured sequentially to avoid spectral bleed-through. Z-stack acquisition and extended depth-of-field fusion were disabled so that all images represented a single focal plane. Exposure time and gain were determined on the fully stained coverslip and held constant across the imaged fields. In the displayed panels, LFNG (Alexa Fluor 647), NOTCH4 (Alexa Fluor 555) and GM130 (Alexa Fluor 488) are shown in yellow, red and green respectively. These colors were assigned for presentation and do not necessarily correspond to the emission wavelengths of the fluorochromes. Because wide-field scanning does not provide optical sectioning and cannot resolve individual Golgi cisternae, no quantitative colocalization analysis was performed, and the images are presented as qualitative evidence of subcellular distribution.

Animal Model and Adenoviral Delivery

Female C57BL/6J mice aged six weeks (Vital River, Beijing, China) were housed under a 12 h light-dark cycle with unrestricted access to food and water and mated overnight with males of the same strain. Detection of a vaginal plug the following morning was recorded as gestational day (GD) 0.5. Twenty-four pregnant females were randomly allocated to four groups of six. The four groups were designated normal control (NC), L-NAME model (PE), L-NAME plus Ad-Lfng (OE) and L-NAME plus empty-vector adenovirus (TC), and these abbreviations are used throughout.

A preeclampsia-like hypertensive phenotype was elicited by subcutaneous Nω-nitro-L-arginine methyl ester (L-NAME; 483125-M, Sigma-Aldrich, St. Louis, MO, USA) dissolved in 0.5% carboxymethylcellulose (C5678, Sigma-Aldrich, St. Louis, MO, USA) and administered once daily at 75 mg/kg from GD11.5 through GD18.5. Control animals received vehicle alone on the same schedule. On GD8.5, mice in the OE group received a single tail-vein injection of 100 µL of a replication-deficient

type 5 adenovirus (E1/E3-deleted) encoding murine Lfng (NM_008494) under the control of a CMV promoter at a titer of 1.15×10^{11} PFU/mL, corresponding to a total dose of 1.15×10^{10} PFU per animal. Mice in the TC group received 100 µL of a control adenovirus (Ad-NC) carrying the identical E1/E3-deleted type 5 backbone and CMV promoter but no Lfng insert, produced and titrated by the same manufacturer in the same batch, at an identical titer and dose. The NC and PE groups received 100 µL of sterile saline. Because the adenovirus was administered on GD8.5 and L-NAME was not begun until GD11.5, the intervention preceded induction of the phenotype by three days. The design was therefore preventive rather than therapeutic and tested whether raising placental Lfng before the insult limited the subsequent development of the phenotype, rather than whether it reversed established disease. Injections were performed with a 29-gauge insulin syringe over approximately 10 s after warming the tail to dilate the vein. Successful placental transduction was confirmed by qRT-PCR, immunoblotting and immunohistochemistry for Lfng in placental tissue. The adenovirus was administered systemically by tail-vein injection, and its biodistribution was not determined. Transduction of the maternal liver, kidney, vasculature, and other tissues therefore cannot be excluded, and the design does not permit the observed effects to be assigned specifically to the placenta.

Systolic and diastolic pressures were recorded by non-invasive tail-cuff plethysmography on alternate days, beginning two days before viral injection. Animals were acclimatized to restraint on three consecutive occasions beforehand, and each recorded value represented the mean of 10 consecutive readings obtained after the trace had stabilized. Mean blood pressure was calculated as diastolic pressure plus one third of the pulse pressure.

At the end of gestation (GD19), dams were deeply anesthetized with pentobarbital sodium (50 mg/kg, i.p.) and euthanized by cervical dislocation. The uterine horns were dissected. Litter size and the number of live fetuses were recorded. Following fetal counting, all surviving fetuses were euthanized by decapitation using sharp surgical scissors in accordance with the approved animal protocol. Death was confirmed by complete decapitation and the absence of cardiac activity and spontaneous respiration. The placentas and kidneys were collected. Portions of each tissue were snap-frozen for qPCR and immunoblotting; the remainder was fixed in 4% paraformaldehyde, embedded in paraffin, and sectioned at 4 µm for hematoxylin-eosin staining and immunohistochemistry as described above.

Statistical Analysis

Analyses were performed in GraphPad Prism (version 10.1.2, GraphPad Software, Boston, MA, USA). Normally distributed variables are presented as mean ± standard deviation and were compared using parametric tests, whereas variables that did not satisfy the normality assumption are presented as median (interquartile range). The number of independent biological replicates differed among assays and is given in each figure legend: n = 3 for western blotting and qRT-PCR validation, colony formation and Transwell assays (Fig. 3A–D,F,G); n = 6 for the CCK-8 growth curves (Fig. 3E); n = 5 for the 2 × 2 factorial $CoCl_2$ experiment (Fig. 5A–C); n = 20 per group for the clinical specimens, with each participant contributing a single value per variable; and n = 6 animals per group for the murine study. Throughout, n denotes independent biological replicates. Technical replicates within an experiment, the qPCR triplicate wells and microscopic fields per section or insert, were averaged before analysis. For the 2 × 2 factorial experiment, each biological replicate comprised a separate cell passage, an independent transfection, an independent $CoCl_2$ exposure, and an independent harvest of RNA and protein, performed on different days. No replicate was derived from subdividing a single transfection or a single treated culture.

Before any parametric test, normality was assessed by the Shapiro-Wilk test and homogeneity of variance by the Brown-Forsythe test. Variables that satisfied the normality assumption were compared by parametric tests, and those that did not were compared by the Mann-Whitney U test. For the *in vitro* and animal experiments, in which the number of independent biological replicates was small (n = 3–6), formal normality testing had limited power, and these data were analyzed parametrically on the assumption of approximate normality. Comparisons between two groups were made by unpaired two-tailed Student's *t*-test. The four murine groups were compared by one-way analysis of variance followed by Tukey's multiple comparisons test. CCK-8 growth curves were analyzed by two-way analysis of variance with treatment and time as factors, followed by Tukey's post-hoc test; only the main effect of treatment was reported. The $CoCl_2$ experiment, which combined two factors at two levels each, was analyzed by two-way analysis of variance with Tukey's post-hoc test. Because the interaction term reached significance for both *NOTCH4* mRNA and NOTCH4 protein, the corresponding main effects were not interpreted, and the pattern was instead described through simple-effect comparisons. A two-sided *p* value below 0.05 was considered significant.

Results

LFNG Is Predicted to Interact With all Four NOTCH Receptors

The preeclamptic placenta undergoes extensive transcriptional reprogramming, and multiple independent transcriptomic studies have documented altered expression of genes governing trophoblast proliferation, invasion and angiogenesis [7]. Among the pathways capable of coordinating such changes in trophoblast behavior, NOTCH signaling is of particular interest because its re-

ceptors are functionally tuned by the Fringe family of β-1,3-N-acetylglucosaminyltransferases (LFNG, MFNG and RFNG), which elongate O-fucose residues on the EGF-like repeats of the receptor ectodomain and thereby influence ligand selectivity. LFNG in particular has been shown to modulate NOTCH receptor activation in prostate, colorectal and pancreatic tumors, and altered NOTCH signaling has been documented in PE placentas. We therefore interrogated the STRING database to determine the predicted relationships between LFNG and the NOTCH receptors. In a network restricted to the Fringe paralogs, the four NOTCH receptors, and selected pathway members, LFNG occupied a central position and was predicted to interact with all four receptors with high confidence, as well as with DLL1, DLL3, JAG1, MESP2, MFNG and RFNG (Fig. 1). Among the four receptors, NOTCH4 is preferentially associated with the vascular endothelium and has been implicated in vascular remodeling, making it particularly relevant to the vascular abnormalities associated with preeclampsia. We therefore focused on the LFNG-NOTCH4 pair and examined its expression directly in clinical PE specimens.

LFNG Is Markedly Reduced and NOTCH4 Is Elevated in Human Preeclamptic Placenta

Placental tissue was obtained from women with PE (n = 20) and from normotensive women delivering at term (n = 20). To verify that sampling captured the intended compartments, serial sections were stained for CD31, CK7 and HLA-G. CD31 showed strong positivity in the vascular endothelium of the villous stroma, CK7 in the cytotrophoblast layer, and HLA-G in interstitial extravillous trophoblast (Fig. 2A), confirming that the sampled regions contained the villous vascular and trophoblastic populations of interest.

Immunohistochemistry revealed distinct cytoplasmic LFNG immunoreactivity in the trophoblast of normotensive placentas, whereas staining was essentially undetectable in PE placentas (Fig. 2B). Morphometric quantification confirmed a profound loss of signal in PE ($p < 0.001$, Fig. 2C). Consistently, qRT-PCR showed that *LFNG* mRNA was reduced in PE placentas relative to the normotensive level ($p < 0.01$, Fig. 2D), whereas *NOTCH4* mRNA was substantially increased in the same specimens ($p < 0.01$, Fig. 2E). All deliveries in both groups occurred at term (≥37 weeks) and were by elective caesarean section performed before the onset of labor. No woman in either group delivered preterm. Gestational age at delivery was 0.50 weeks lower in the preeclamptic group (38.64 [38.00–39.40] vs 39.14 [38.71–39.57] weeks), and the two distributions overlapped substantially (Table 1). Thus, loss of LFNG and accumulation of NOTCH4 occur concurrently in the PE placenta, indicating an inverse association between the two molecules in diseased tissue.

LFNG Overexpression Enhances Trophoblast Proliferation and Invasion

Because deficient trophoblast proliferation and invasion underlie the inadequate spiral artery remodeling that characterizes PE, we asked whether increasing LFNG was sufficient to improve these functions. Western blotting first confirmed that endogenous LFNG protein was expressed at comparable levels in the immortalized extravillous trophoblast line HTR-8/SVneo and the choriocarcinoma line JAR (Fig. 3A), making both suitable for gain-of-function studies. Cells were transfected with an LFNG expression plasmid (OE-LFNG) or the corresponding empty vector (OE-NC). Overexpression was confirmed at the protein level in HTR-8/SVneo ($p < 0.001$, Fig. 3B) and in JAR ($p < 0.001$, Fig. 3C), and at the transcript level in both lines (both $p < 0.001$, Fig. 3D).

CCK-8 assays performed at 24, 48, 72 and 96 h showed that LFNG overexpression accelerated the growth of both cell lines, with the difference becoming progressively more pronounced over time (main effect of treatment by two-way analysis of variance (ANOVA), $p < 0.01$ in HTR-8/SVneo and $p < 0.05$ in JAR, Fig. 3E). Colony formation assays were concordant. Colony numbers increased in HTR-8/SVneo ($p < 0.01$) and JAR ($p < 0.001$, Fig. 3F). In Matrigel-coated Transwell assays, LFNG overexpression increased invasive capacity in both lines, with greater numbers of invaded cells per field in HTR-8/SVneo ($p < 0.05$) and JAR ($p < 0.001$, Fig. 3G). LFNG therefore positively regulates both the proliferative and invasive behavior of trophoblast cells, two functions that are impaired in PE. These assays were performed under standard culture and without manipulation of NOTCH4 and therefore identify LFNG as a positive regulator of trophoblast behavior without establishing that these effects are mediated through NOTCH4.

LFNG and NOTCH4 Share a Golgi-Associated Perinuclear Distribution

We next examined the relationship between LFNG and NOTCH4. Western blotting showed that endogenous NOTCH4 protein was expressed at similar levels in HTR-8/SVneo and JAR cells (Fig. 4A). An expanded STRING network centered on LFNG and NOTCH4 placed the two proteins within a densely interconnected module that also contained the remaining Fringe paralogs, the O-glycosyltransferases POFUT1 and POGLUT1, the ligands DLL1 and DLL3, the DTX1-DTX4 ubiquitin ligases and the canonical downstream effectors HES5, HEY1, HEY2 and NRARP (Fig. 4B), consistent with a potential glycosylation-dependent regulatory relationship.

Fringe glycosyltransferases modify NOTCH receptors during their transit through the secretory pathway, so LFNG and NOTCH4 would be expected to encounter one another in the Golgi apparatus. HTR-8/SVneo cells were therefore stained simultaneously for LFNG, NOTCH4 and the cis-Golgi marker GM130, using primary antibodies raised

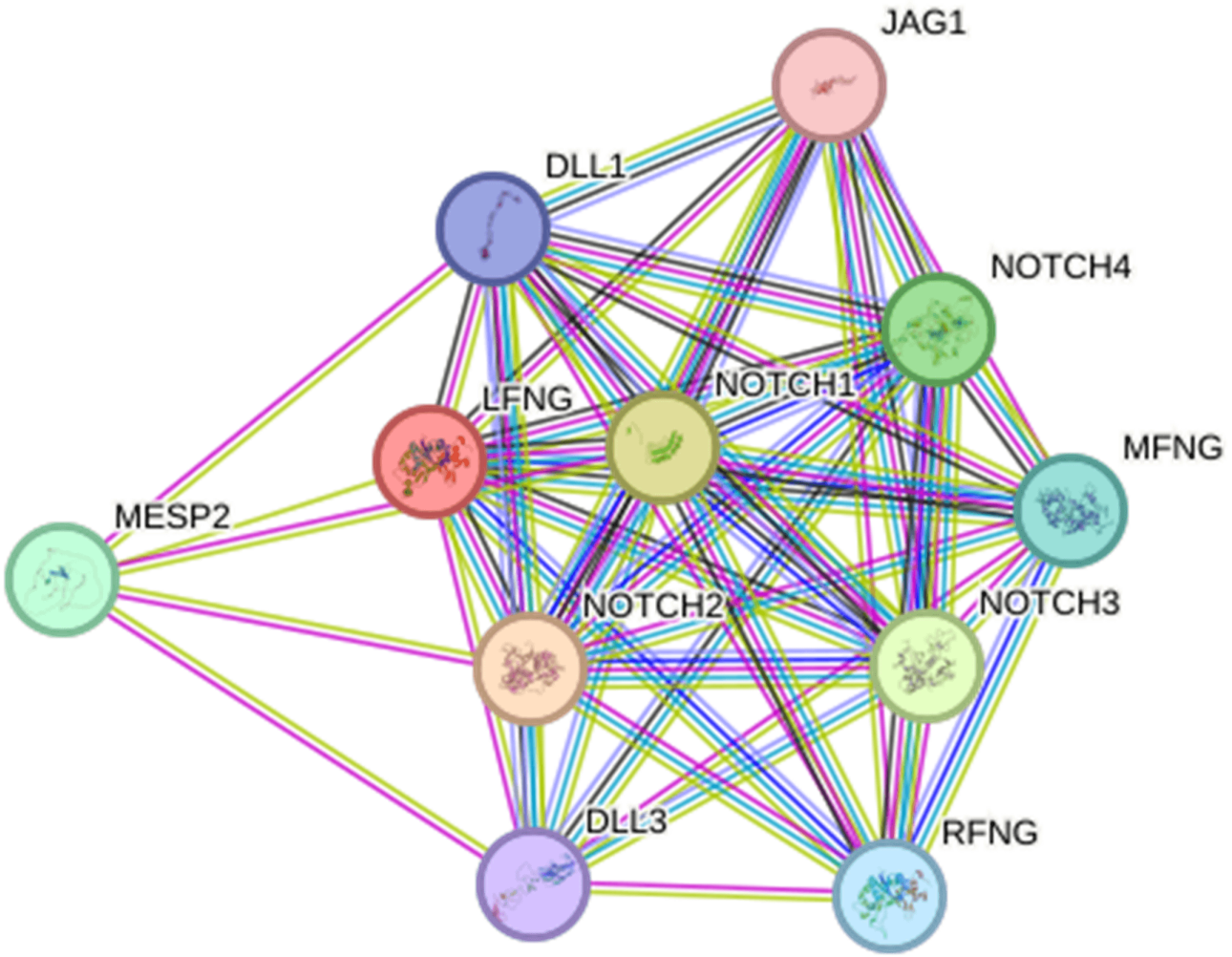

Fig. 1. LFNG is predicted to interact with all four NOTCH receptors. Protein-protein interaction network of the Fringe family (LFNG, MFNG, RFNG), the four NOTCH receptors and selected pathway members, constructed in STRING. Nodes represent proteins and edges represent predicted or experimentally supported associations, with edge color denoting the type of evidence. LFNG was predicted to interact with all four NOTCH receptors with high confidence (combined scores: NOTCH1, 0.973; NOTCH2, 0.979; NOTCH3, 0.969; NOTCH4, 0.938).

in three different host species and detected with species-specific cross-adsorbed secondary antibodies (Fig. 4C). LFNG and GM130 were both finely granular, cytoplasmic and accentuated in the juxtanuclear region, and their signals overlapped across much of the cytoplasm. NOTCH4, detected in these images with a different antibody directed against the intracellular domain, was present throughout the cytoplasm and was additionally enriched within the nucleus in the majority of cells, as expected for a reagent that recognizes both the full-length receptor and the released intracellular domain. In the merged images, the cytoplasmic LFNG, NOTCH4 and GM130 signals coincided, whereas the nuclear NOTCH4 signal showed no corresponding LFNG or GM130 signal.

The cytoplasmic pools of LFNG and NOTCH4 therefore share a distribution with the cis-Golgi marker, consistent with the two proteins being co-resident in the Golgi, while the nuclear NOTCH4 signal is consistent with the presence of the released intracellular domain. These images document a shared subcellular distribution but do not resolve individual Golgi cisternae and were not used to derive a quantitative measure of colocalization.

LFNG Regulates NOTCH4 Abundance in a Cell-State-Dependent Manner, Without Affecting HIF-1α

The PE placenta is characterized by ischemia and hypoxia, whereas cultured trophoblasts are typically maintained under ambient oxygen conditions. To determine whether a hypoxia-like cellular state alters the LFNG-NOTCH4 relationship, we performed a 2 × 2 factorial experiment in HTR-8/SVneo cells, combining LFNG overexpression with chemical hypoxia induced by $CoCl_2$ (150 μM, 24 h). $CoCl_2$ stabilizes HIF-1α and recapitulates the

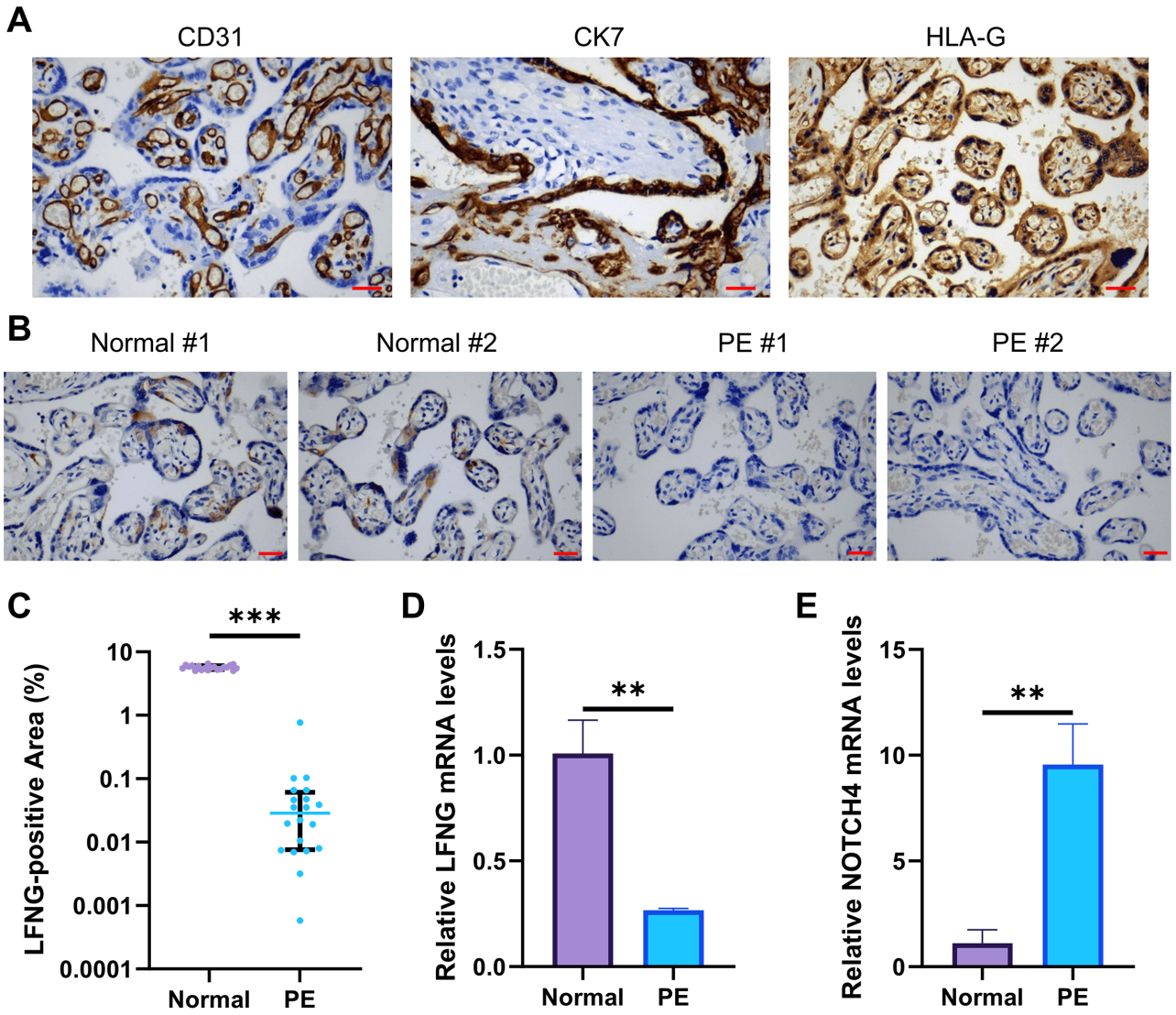

Fig. 2. LFNG is markedly reduced and NOTCH4 is elevated in human preeclamptic placenta. (A) Immunohistochemical validation of the sampled compartments in placental tissue, including CD31 in villous stromal vascular endothelium, CK7 in the cytotrophoblast layer and HLA-G in interstitial extravillous trophoblast, all strongly positive. Scale bar, 100 µm. (B) Representative immunohistochemical staining for LFNG in placental tissue from two normotensive term pregnancies (Normal #1, #2) and two women with preeclampsia (PE #1, #2). LFNG showed distinct cytoplasmic staining in villous trophoblast of normotensive placentas and was essentially undetectable in PE. Scale bar, 100 µm. (C) Morphometric quantification of the LFNG-positive area, with each symbol representing one specimen (n = 20 per group). (D,E) qRT-PCR analysis of *LFNG* (D) and *NOTCH4* (E) mRNA in the same specimens, normalized to GAPDH and expressed relative to the normotensive group (n = 20 per group). In (C), the LFNG-positive area was not normally distributed in the preeclampsia group (Shapiro-Wilk $p < 0.001$) and is shown as the median with interquartile range and compared by the Mann-Whitney U test. Note the logarithmic scale of the y axis. $^{**}p < 0.01$, $^{***}p < 0.001$. PE, preeclampsia.

HIF-dependent arm of the hypoxic response; however, it is a chemical mimetic and does not substitute for culture under low oxygen tension.

Successful induction of a hypoxia-like state was confirmed by marked stabilization of HIF-1α in both $CoCl_2$-treated groups (Fig. 5B,C). For HIF-1α, two-way ANOVA showed a significant main effect of $CoCl_2$ ($F(1,16) = 6129$, $p < 0.0001$) but no effect of LFNG ($F(1,16) = 0.97$, $p > 0.05$) and no interaction between the two factors ($F(1,16) = 0.12$, $p > 0.05$; Fig. 5C). Post-hoc comparisons confirmed that LFNG overexpression did not alter HIF-1α levels under either standard culture conditions or $CoCl_2$ treatment (both $p > 0.05$; Fig. 5B,C). In contrast, the effect of LFNG on NOTCH4 differed markedly between standard culture conditions and the $CoCl_2$-induced hypoxia-like state. Two-way ANOVA revealed a highly significant interaction be-

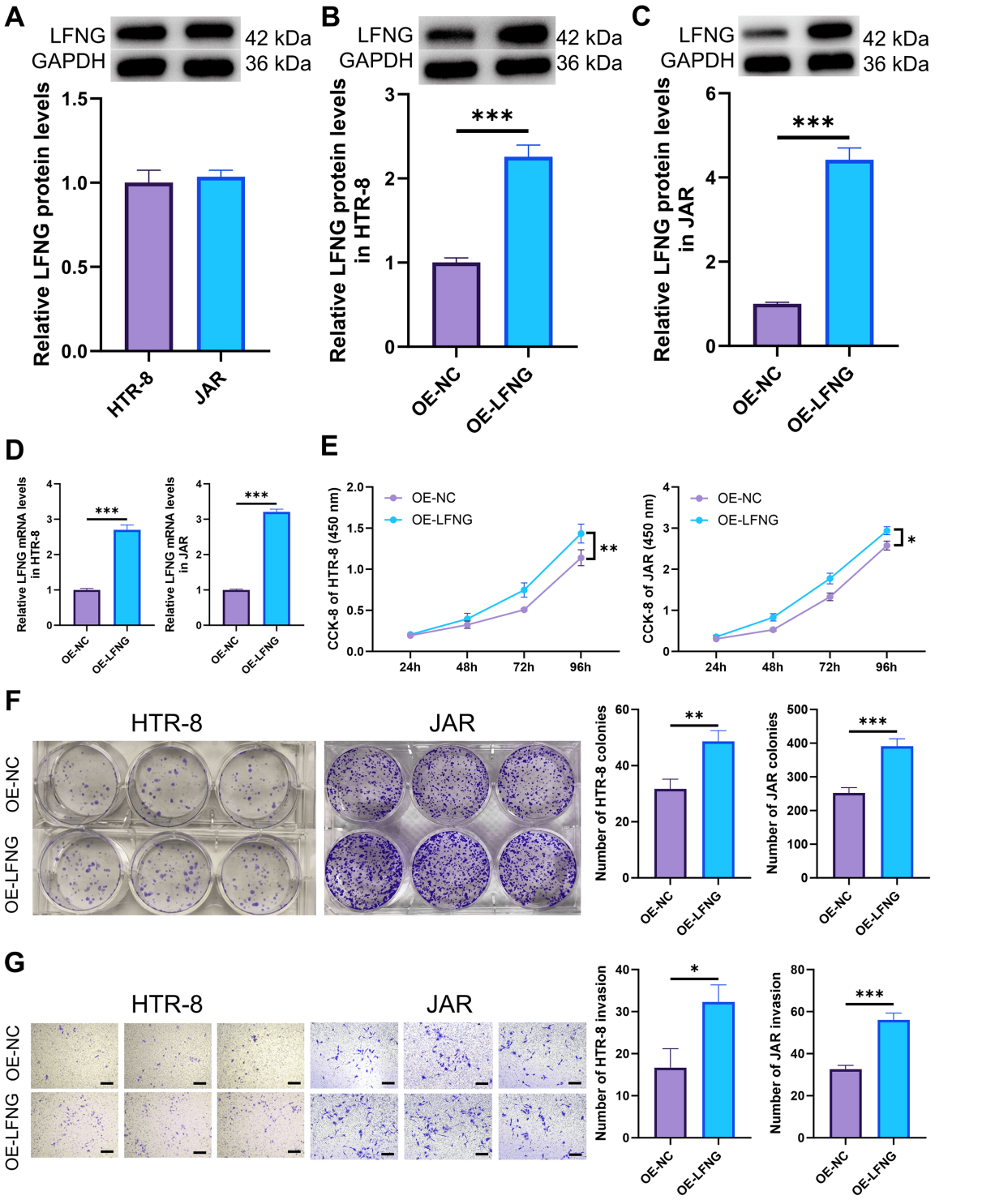

Fig. 3. LFNG overexpression promotes trophoblast proliferation and invasion. (A) Western blot of endogenous LFNG in HTR-8/SVneo and JAR cells, with GAPDH as loading control, densitometry expressed relative to HTR-8/SVneo (n = 3). (B,C) Validation of LFNG overexpression at the protein level in HTR-8/SVneo (B) and JAR (C) cells transfected with an LFNG expression plasmid (OE-LFNG) or empty vector (OE-NC) (n = 3). (D) qRT-PCR validation of *LFNG* overexpression in HTR-8/SVneo (left) and JAR (right) cells, normalized to *GAPDH* (n = 3). (E) CCK-8 assay of HTR-8/SVneo (left) and JAR (right) cells at 24, 48, 72 and 96 h after transfection, absorbance measured at 450 nm (n = 6). (F) Representative images and quantification of colony formation in HTR-8/SVneo and JAR cells (n = 3). (G) Representative images and quantification of Matrigel-coated Transwell invasion assays after 24 h (n = 3). Scale bar, 100 μm. Data are mean ± SD, n for each panel is indicated above. Comparisons in (A–D,F,G) by unpaired two-tailed Student's *t*-test and in (E) by Two-way analysis of variance (ANOVA) (main effect of treatment). *$p < 0.05$, **$p < 0.01$, ***$p < 0.001$.

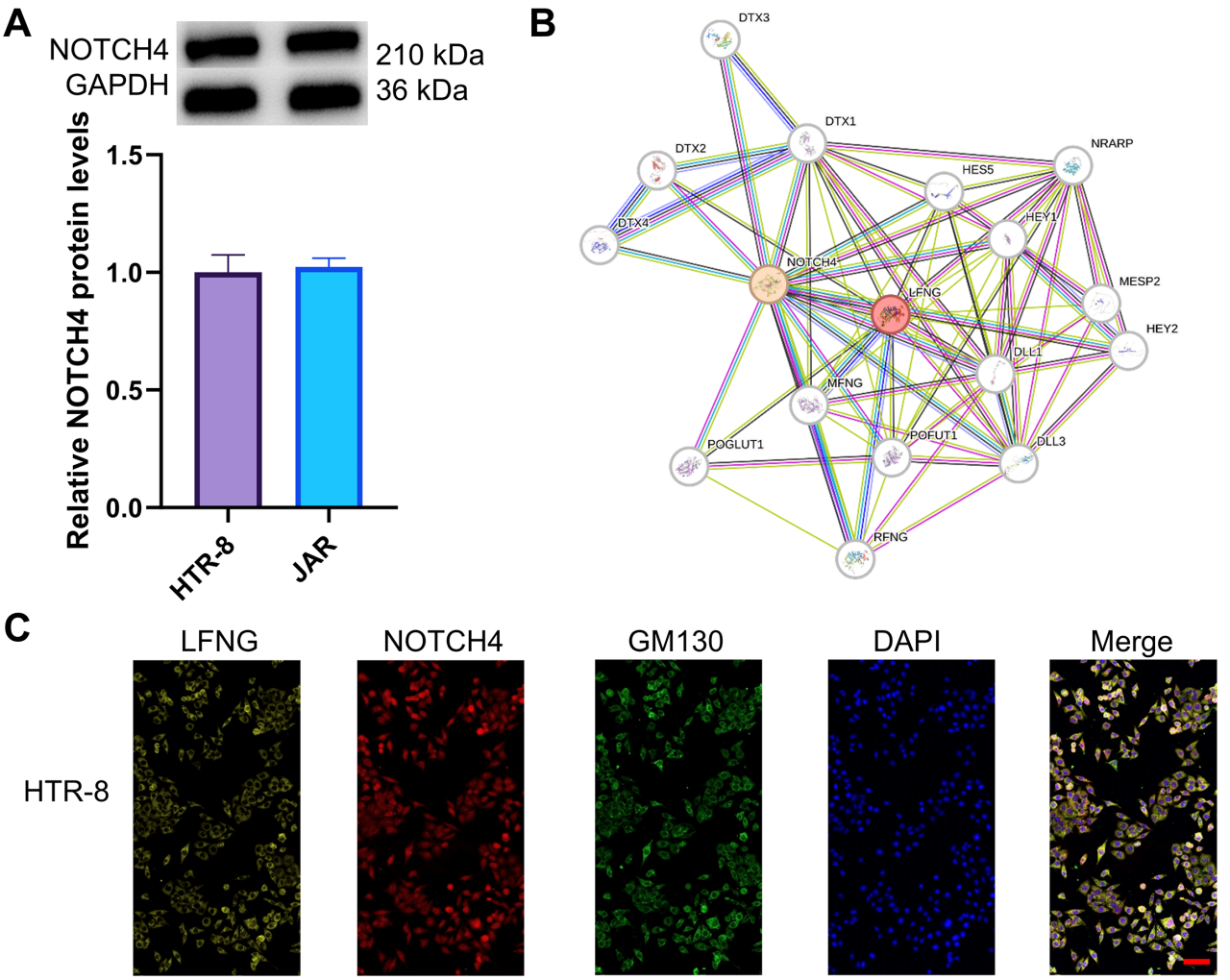

Fig. 4. LFNG and NOTCH4 share a Golgi-associated perinuclear distribution. (A) Western blot of endogenous NOTCH4 in HTR-8/SVneo and JAR cells, with GAPDH as loading control, densitometry expressed relative to HTR-8/SVneo. (B) Expanded STRING network centered on LFNG and NOTCH4. (C) Representative immunofluorescence images of HTR-8/SVneo cells stained for LFNG (yellow), NOTCH4 (red), the cis-Golgi marker GM130 (green) and DAPI (blue), together with the merged image. Display colors are assigned for presentation and do not necessarily correspond to the emission wavelength of the fluorochrome. Staining was performed in three independent experiments. Representative images from one coverslip are shown, all panels being from the same field and a single focal plane acquired by wide-field scanning without optical sectioning. Scale bar, 100 µm. Data in (A) are mean ± SD from 3 independent experiments, comparison by unpaired two-tailed Student's *t* test.

tween LFNG overexpression and $CoCl_2$ treatment for both *NOTCH4* mRNA ($F(1,16) = 1243$, $p < 0.0001$; Fig. 5A) and NOTCH4 protein ($F(1,16) = 891.6$, $p < 0.0001$; Fig. 5B,C). Because the interaction was significant, the main effects were not interpreted, and the pattern was instead defined by post-hoc comparisons. Under standard culture conditions, LFNG overexpression increased *NOTCH4* mRNA ($p < 0.001$, Fig. 5A) and NOTCH4 protein ($p < 0.001$, Fig. 5B,C) relative to OE-NC. $CoCl_2$ treatment alone induced increases of comparable magnitude at both levels (both $p < 0.001$, Fig. 5A–C), recapitulating *in vitro* the NOTCH4 accumulation observed in PE placentas. Critically, when the two stimuli were combined, their effects were not additive but opposing. In $CoCl_2$-treated cells, LFNG overexpression reduced *NOTCH4* mRNA and protein levels to values significantly below those observed with $CoCl_2$ treatment alone (both $p < 0.001$), although both remained significantly higher than the standard-culture control levels (both $p < 0.001$, Fig. 5A–C). Thus, the direction of the effect of LFNG on NOTCH4 abundance depended on the cellular state, being positive under standard culture conditions and negative under $CoCl_2$ treatment. Possible explanations for this reversal are considered in the Discussion.

Because GAPDH is a recognized HIF-1 target gene, we confirmed that it remained a valid normalizer under these conditions. Raw GAPDH Cq values and GAPDH

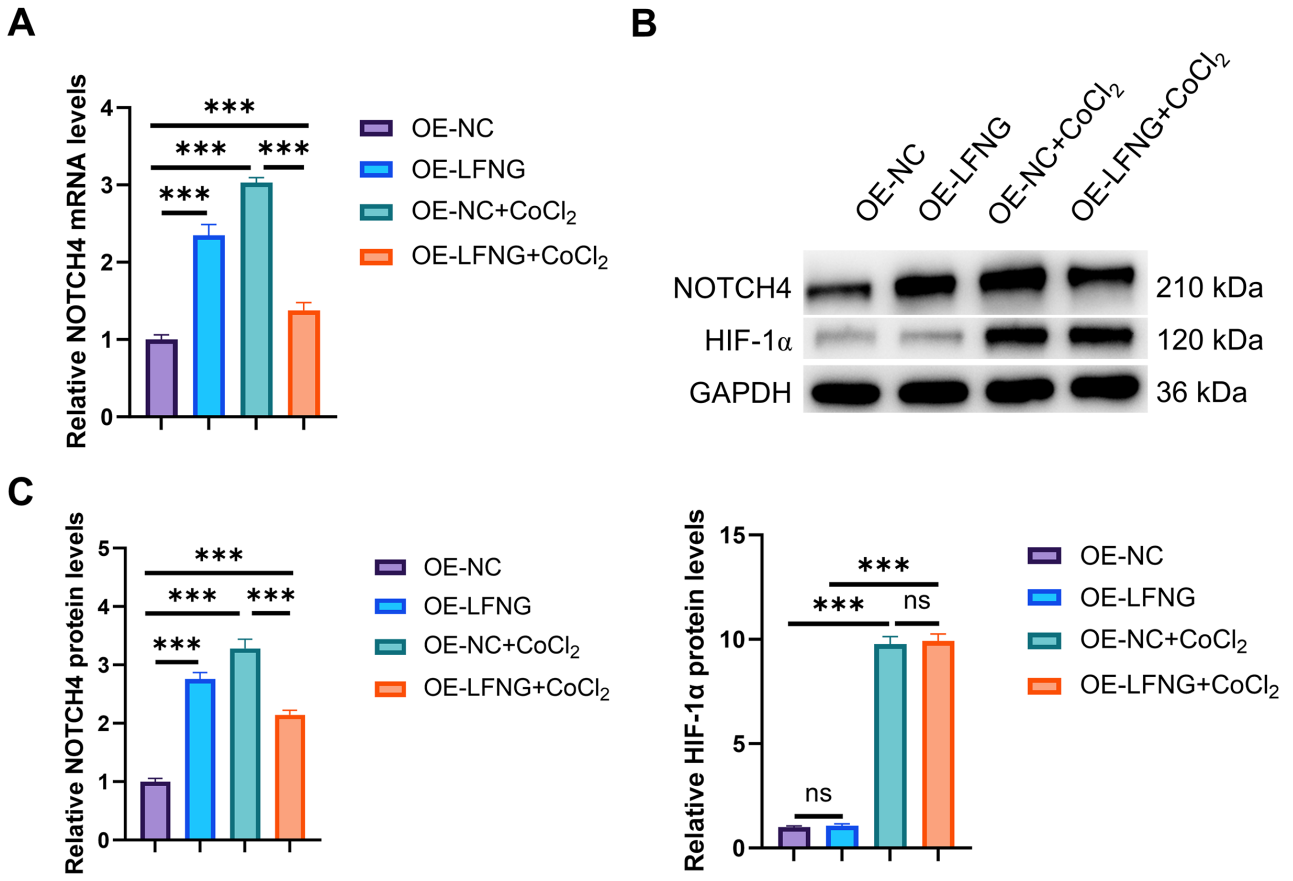

Fig. 5. LFNG regulates NOTCH4 abundance in a cell-state-dependent manner, without affecting HIF-1α. (A) qRT-PCR analysis of *NOTCH4* mRNA in HTR-8/SVneo cells subjected to a 2 × 2 factorial design combining LFNG overexpression with chemical hypoxia ($CoCl_2$, 150 μM, 24 h), normalized to *GAPDH* and expressed relative to OE-NC. (B) Representative western blots of NOTCH4 and HIF-1α in the same four groups, with GAPDH as loading control. (C) Corresponding densitometric quantification. Data are mean ± SD from five independent experiments. Comparisons in (A) and (C) by two-way ANOVA followed by Tukey's multiple comparisons test. ***$p < 0.001$; ns, not significant.

band densities at equal total-protein loading were closely comparable across the four conditions and showed no evidence of HIF-driven induction (all pairwise $p > 0.05$; **Supplementary Fig. 1A,B**). As a further check independent of any reference gene, raw NOTCH4 Cq values obtained from a fixed input of total RNA were analyzed directly and reproduced the same interaction ($F(1,16) = 848.2$, $p < 0.0001$, accounting for 88.55% of the total variation) and the same post-hoc pattern (**Supplementary Fig. 1C**). The residual standard deviation of the assay was 0.088 cycles, corresponding to a coefficient of variation of approximately 6%, indicating that the magnitude of the F statistics reflects the size of the effect rather than unusually low measurement variability. Numerical details are provided in the legend to **Supplementary Fig. 1**.

Raising LFNG therefore does not amplify the effect of $CoCl_2$ but instead blunts it, partially attenuating the $CoCl_2$-driven increase in NOTCH4 while leaving HIF-1α stabilization intact. The reversal in the direction of the LFNG effect between standard culture conditions and a $CoCl_2$-induced hypoxia-like state indicates that the consequence of LFNG activity on NOTCH4 depends on the cellular state in which it is measured. This provides a possible explanation for the positive effect of LFNG on NOTCH4 under standard culture conditions and the inverse relationship observed in the hypoxic PE placenta, although $CoCl_2$ reproduces only part of the response to genuine low oxygen conditions. Both readouts reflect the abundance of NOTCH4 transcript and NOTCH4 protein. The cleaved intracellular domain and canonical Notch target genes were not measured; therefore, these experiments document changes in receptor abundance rather than changes in Notch pathway output.

Preventive Lfng Delivery Limits the Development of Preeclampsia-Like Phenotypes and Normalizes Placental Notch4 in Mice

To test whether the relationship between LFNG and NOTCH4 is relevant *in vivo*, a PE-like hypertensive phenotype was induced in pregnant C57BL/6J mice by subcutaneous L-NAME (75 mg/kg/day, GD11.5-GD18.5). Four

groups were studied (n = 6 each), including normal control (NC), L-NAME alone (PE), L-NAME plus tail-vein injection of an Lfng-expressing adenovirus on GD8.5 (OE), and L-NAME plus an equivalent dose of control adenovirus (TC). Because the adenovirus was given on GD8.5, three days before L-NAME was begun, the experiment tests prevention of the phenotype rather than treatment of established disease.

L-NAME reproduced the cardinal features of the model. Mean blood pressure was higher in the PE group than in NC mice ($p < 0.001$, Fig. 6A), and the number of live fetuses was correspondingly lower ($p < 0.001$, Fig. 6C). Litter size showed the same trend, but this difference did not reach significance. Among the L-NAME-treated groups, only the TC group had a significantly lower litter size than the NC group ($p < 0.05$, Fig. 6B). The TC group was indistinguishable from the PE group for every parameter, excluding a non-specific effect of adenoviral infection. Prior adenoviral delivery of Lfng limited the development of the phenotype relative to the vector control. Mean blood pressure was lower in the OE group than in TC mice ($p < 0.001$, Fig. 6A), and the number of live fetuses was higher ($p < 0.05$, Fig. 6C). Litter size was higher in the OE group than in the TC group, but the difference did not reach significance (Fig. 6B). Both blood pressure and live fetal number in the OE group remained significantly different from NC (both $p < 0.001$), indicating partial rather than complete protection.

Placentas from PE and TC mice showed a densely packed labyrinth with increased infarct-like nodules, congested, fragmented and necrotic villi, and narrowed vascular lumina with thickened intervillous septa. In the OE group, nodules were sparse and only limited villous congestion and mild luminal narrowing remained (Fig. 6D). Renal sections from PE and TC animals displayed swollen and hyperplastic glomerular capillary endothelium with narrowed lumina, expanded matrix, loosened architecture, and scattered lymphomonocytic infiltration, whereas OE kidneys retained a comparatively compact architecture with only mild endothelial swelling and occasional inflammatory cells (Fig. 6E).

At the molecular level, the reciprocal relationship observed in human placenta was recapitulated, but with an instructive asymmetry. Placental *Lfng* mRNA and protein were both markedly reduced in the PE group relative to NC (both $p < 0.001$; Fig. 6F,G). In animals given Ad-Lfng before L-NAME, these values were higher than in TC (both $p < 0.001$ vs. TC), although they nevertheless remained significantly below NC (both $p < 0.001$; Fig. 6F,G). *Notch4* mRNA and protein, by contrast, were increased in the PE group (both $p < 0.001$) and remained at control values after Lfng delivery ($p < 0.001$ vs. TC), with no significant difference from NC (both $p > 0.05$; Fig. 6F,G). Lfng, which was abundant and homogeneously distributed in the labyrinth layer and trophoblast of NC placentas, was markedly reduced and unevenly distributed in the PE and TC groups and was partially preserved in the OE group ($p < 0.001$ vs. TC and vs. NC) (Fig. 6H).

Taken together, prior delivery of Lfng limited the development of the phenotype and kept placental Notch4 at control values, consistent with the suppression of $CoCl_2$-driven NOTCH4 induction observed in trophoblast cells (Fig. 5A–C). Because the adenovirus was given intravenously, the molecular effect documented here was measured in the placenta, whereas the maternal and fetal phenotypic improvements cannot be attributed to the placenta alone. The dissociation between complete normalization of Notch4 and only partial correction of Lfng levels, blood pressure, and fetal outcome suggests that NOTCH4 is a necessary but not sufficient node in this pathway, and that additional Lfng-independent consequences of NOS inhibition contribute to the phenotype.

Discussion

The present study shows that LFNG, a component of the placental Notch machinery, is markedly reduced in preeclampsia. Three lines of evidence converge on this conclusion. In clinical specimens, both LFNG protein and transcript levels were markedly reduced in PE placentas, whereas *NOTCH4* mRNA increased almost tenfold in the same tissue. In trophoblast cells, LFNG overexpression enhanced proliferation, colony formation, and Matrigel invasion. In pregnant mice, adenoviral delivery of Lfng before model induction limited the rise in blood pressure, preserved fetal survival, reduced placental and renal injury, and maintained placental Notch4 at control levels. These observations place a Golgi glycosyltransferase, a class of enzyme rarely considered in the context of placental disease, within the pathophysiology of preeclampsia.

The relevance of LFNG to placental function is supported by its established biochemical roles. Fringe enzymes extend selected O-fucose glycans installed by POFUT1 on the EGF-like repeats of the Notch ectodomain with a β1,3-linked N-acetylglucosamine [17], thereby modulating ligand selectivity and, in many receptor-ligand contexts, enhancing Delta-like signaling while attenuating Jagged-mediated activation [23]. Because Notch signaling regulates trophoblast progenitor maintenance and lineage differentiation [16], and has been implicated in endovascular trophoblast invasion and trophoblast-dependent spiral artery remodeling [22], an enzyme that sets receptor ligand preference is well positioned to influence precisely those processes that fail in preeclampsia. Our functional data are consistent with this expectation. LFNG gain of function improved both the proliferative and invasive behavior of trophoblast cells, two capacities whose deficiency underlies shallow placentation.

A more difficult question is how a glycosyltransferase that acts post-translationally comes to alter NOTCH4 transcript abundance, as shown in Fig. 5A. LFNG cannot plau-

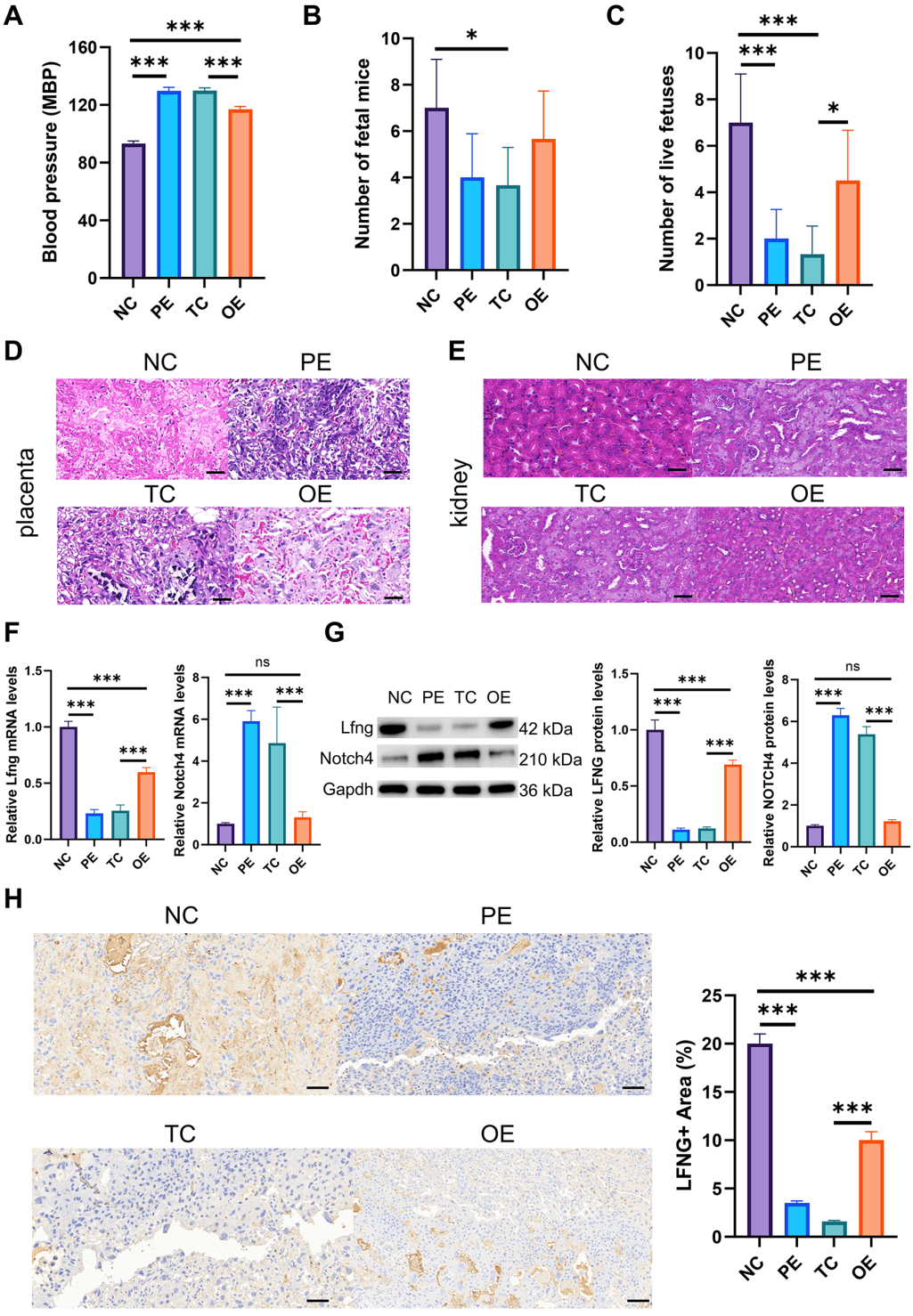

Fig. 6. Preventive Lfng delivery limits the development of preeclampsia-like phenotypes and normalizes placental Notch4 in mice. (A) Mean blood pressure measured by tail-cuff plethysmography on GD18.5. (B) Number of fetuses per litter. (C) Number of live fetuses per litter. (D) Representative hematoxylin and eosin staining of placental sections. (E) Representative hematoxylin and eosin staining of renal sections. Scale bar, 100 μm. (F) qRT-PCR analysis of placental *Lfng* (left) and *Notch4* (right) mRNA, normalized to *Gapdh* and expressed relative to NC. (G) Representative western blots of placental Lfng and Notch4, with Gapdh as loading control, and corresponding densitometric quantification. (H) Representative immunohistochemical staining for Lfng in placental sections and quantification of the LFNG-positive area. Scale bar, 100 μm. Data are mean ± SD, n = 6 mice per group; comparisons by one-way ANOVA followed by Tukey's multiple comparisons test. *$p < 0.05$, ***$p < 0.001$; ns, not significant.

sibly bind the NOTCH4 promoter, and we do not propose that it does. The most economical explanation involves the transcriptional feedback built into Notch signaling itself. Ligand engagement liberates NICD, which induces the HES and HEY families of transcriptional repressors together with NRARP [31]. HEY proteins repress a broad set of targets, while NRARP promotes NICD turnover, such that pathway output is continuously fed back onto pathway components [32]. By changing the glycosylation state of the receptor ectodomain, LFNG alters the efficiency with which ligand engagement is converted into NICD, and a change in feedback tone could reasonably be transmitted to NOTCH4 transcription. It should be stated plainly that this remains an inference. What we measured was the abundance of NOTCH4 transcript and protein, which reflects receptor expression rather than pathway activity. We did not quantify the cleaved intracellular domain of NOTCH4 or the canonical target genes HES1, HES5, HEY1, HEY2 and NRARP, and have therefore avoided describing our findings as evidence of altered Notch signaling. Whether the loss of LFNG observed in preeclamptic placenta translates into altered Notch output remains to be determined. This could be addressed most directly by immunoblotting for the cleaved intracellular domain using a neo-epitope-specific antibody, by a Notch-responsive reporter assay, and by quantifying these target genes under both standard culture conditions and a hypoxia-like state. The evidence linking LFNG to NOTCH4 in this study rests on their shared subcellular distribution and database prediction rather than on biochemical evidence such as co-immunoprecipitation or site-resolved glycosylation analysis. Directly establishing this molecular link and connecting it to pathway output is the natural next step.

The reversal of the LFNG effect between culture conditions deserves particular comment, as it is the most unusual feature of our data. Under ambient oxygen, LFNG overexpression increased NOTCH4. In a $CoCl_2$-induced hypoxia-like state, however, the same manipulation attenuated this induction, reducing NOTCH4 relative to $CoCl_2$ alone while leaving it above the standard-culture control. The interaction term accounted for most of the variance in both mRNA and protein, indicating that the change in direction is not a marginal statistical artifact. HIF-1α stabilization was entirely unaffected by LFNG, placing LFNG downstream of, or parallel to, HIF-1α stabilization rather than upstream of it. Hypoxia can alter Notch output through multiple HIF-dependent and HIF-independent mechanisms. In some cellular contexts, stabilized HIF-1α physically associates with NICD and potentiates Notch output [33]. However, the functional consequences of hypoxia-Notch crosstalk depend on cell type and experimental conditions [34], and it is conceivable that the abundance of a fringe enzyme influences how this amplification is resolved. We cannot, however, distinguish among the possible mechanisms with the present data. What this finding does accomplish is to reconcile an apparent contradiction. Standard culture at atmospheric oxygen is a poor surrogate for the ischemic intervillous space, and the positive LFNG-NOTCH4 relationship observed under standard culture conditions therefore need not conflict with the inverse relationship observed in diseased tissue. Notably, the murine placenta, in which hypoxia arises from genuine placental ischemia rather than from a chemical mimetic, shows the same pattern. This lends support to the interpretation that a low-oxygen environment, rather than cobalt itself, underlies the reversal.

Adenoviral Lfng preserved placental Lfng only partially, at roughly 60–70% of control levels, yet Notch4 remained at control values, with no residual difference from NC mice. Blood pressure and live fetal number improved significantly but remained well below normal. Notch4 therefore appears sensitive to comparatively modest changes in Lfng, such that incomplete preservation of the enzyme is sufficient to maintain the receptor at control levels. More importantly, however, correction of Notch4 was clearly not equivalent to correction of the phenotype. Notch4 is therefore best regarded as a necessary but not sufficient node. This incomplete protection is not unexpected given the model used, because systemically administered L-NAME inhibits nitric oxide synthase throughout the maternal circulation and induces endothelial, renal, and hemodynamic disturbances that an intervention acting principally through a single glycosyltransferase may not fully prevent [35].

Several limitations bear emphasis. The first concerns the causal architecture of the relationship. Our design establishes that LFNG overexpression alters NOTCH4 abundance and, separately, enhances trophoblast proliferation, colony formation, and invasion, but it does not establish that the latter effects follow from the former. Indeed, the two effects are dissociated in the assays that demonstrate them, since the functional experiments were performed under standard culture conditions, in which LFNG increases rather than decreases NOTCH4. A model in which suppression of NOTCH4 mediates the functional benefit of LFNG is therefore not supported by our own data, and we do not propose such a mechanism. Rather, we report the two effects as parallel findings without inferring mediation. Demonstrating that the functional consequences of LFNG are transmitted through NOTCH4 would require an epistasis design that was not performed in the present study. Such experiments could include NOTCH4 knockdown by siRNA or shRNA, or pharmacological inhibition of Notch cleavage, in LFNG-overexpressing cells, together with reciprocal rescue by re-expression of NOTCH4 in the same background, with proliferation and invasion assessed under both standard culture conditions and a hypoxia-like state. Until such experiments are performed, the relationship between LFNG and NOTCH4 should be regarded as two associated effects rather than as a demonstrated linear pathway.

$CoCl_2$ reproduces HIF stabilization but not the full cellular response to low oxygen [36], and it can exert additional cobalt-specific effects on oxidative stress and calcium-dependent signaling that may be partly independent of HIF [37]. The *in vitro* experiments therefore establish that the direction of the LFNG effect on NOTCH4 depends on the cellular state induced by $CoCl_2$, rather than on oxygen tension per se. Confirmation would require culture at a physiological oxygen tension of 1–3% O_2, and we have accordingly avoided describing the *in vitro* finding as oxygen-dependent. The observation that the same reciprocal relationship is present in the murine placenta, where hypoxia arises from genuine placental ischemia, is consistent with a true low-oxygen effect but does not substitute for this direct experiment. We did not undertake a formal multi-gene reference validation. Normalization under chemical hypoxia instead rests on the stability of GAPDH demonstrated directly under our experimental conditions at both the transcript and protein levels, together with analysis of raw Cq values obtained from a fixed input of total RNA and therefore independent of any reference gene. The subcellular localization data are also qualitative. Imaging was performed by wide-field fluorescence scanning, which lacks optical sectioning. Out-of-focus signal from other cellular planes is superimposed on the plane of interest, and wide-field imaging cannot resolve individual Golgi cisternae. For these reasons, we deliberately refrained from calculating correlation coefficients, which would be systematically biased upward under these acquisition conditions, and restrict our claim to a shared perinuclear distribution rather than colocalization at the organelle level. Confocal or super-resolution imaging, together with biochemical approaches such as co-immunoprecipitation or subcellular fractionation, will be required to establish whether LFNG and NOTCH4 physically associate within the Golgi. HTR-8/SVneo is a heterogeneous cell line containing cells with mesenchymal characteristics, and JAR is choriocarcinoma-derived [38]; neither fully represents primary extravillous trophoblast. The clinical cohort was modest (twenty case–control pairs) and drawn from a single center, and we measured NOTCH4 alone rather than surveying all four receptors. Finally, the adenovirus was administered three days before L-NAME, so the murine experiment establishes that increasing placental Lfng limits development of the phenotype but does not test whether the enzyme can modify disease once established. Whether Lfng delivery after the onset of hypertension confers benefit remains to be determined and would be the appropriate design for assessing therapeutic rather than preventive value.

Several clinical characteristics other than blood pressure differed between the groups and could, in principle, influence placental LFNG or NOTCH4 expression. Parity was identical in median and interquartile range, whereas gravidity was lower in the preeclamptic group, consistent with the established excess of first pregnancies among women with preeclampsia. We are not aware of evidence that either variable regulates Notch signaling in the term placenta. Birth weight was lower in the preeclamptic group by a median of 0.20 kg, although the interquartile ranges in both groups remained within the normal range for term infants. Reduced fetal growth in preeclampsia is itself a recognized consequence of impaired placental function, so birth weight is better regarded as part of the disease phenotype than as an independent determinant of LFNG expression; adjusting for it would therefore risk removing part of the effect under study. The laboratory variables were closely similar between the groups (Table 1).

Gestational age at delivery was slightly lower in the preeclamptic group, by a median of 0.50 weeks. Because the study was restricted to elective caesarean deliveries performed before the onset of labor, both groups delivered at term and their gestational age distributions overlapped substantially. The cohort therefore does not carry the imbalance that arises when preeclamptic cases requiring iatrogenic preterm delivery are compared with term controls. The magnitude of the difference is also difficult to reconcile with a maturational explanation. Attributing the near-total loss of LFNG, from a median of 5.68% to 0.03% of villous area, a reduction of more than 99%, to a difference of only three and a half days at term would require the enzyme to decline with a half-life of approximately eleven hours in the normal placenta, a rate incompatible with the gradual maturational changes described in third-trimester villous trophoblast. Two further observations argue against maturation. First, the same reciprocal relationship between Lfng and Notch4 was reproduced in mice examined on a single gestational day, a design in which gestational age was identical across groups by construction. Second, the direction of the LFNG effect on NOTCH4 was reversed in a $CoCl_2$-induced hypoxia-like state *in vitro*, under conditions in which gestational age plays no part. We nevertheless acknowledge that LFNG and NOTCH4 expression were not examined in relation to individual clinical covariates and that, with only twenty women per group, the study would in any case have had limited power for such adjustment. A contribution from gestational age, gravidity, or birth weight therefore cannot be formally excluded. Because all cases delivered at term, the cohort is also weighted toward the milder end of the disease spectrum, and the association between LFNG and disease severity could not be assessed. A larger cohort with prospectively recorded covariates, including women with early-onset preeclampsia and a gestational-age-matched preterm control group, will be needed to address these questions.

Finally, urinary protein was not assessed in the mice, which is why the model is described throughout as a preeclampsia-like hypertensive phenotype rather than as preeclampsia proper. The route of adenoviral delivery imposes a further important limitation on interpretation. The virus was administered by tail-vein injection, and type 5

adenovirus given intravenously is known to transduce the liver efficiently, as well as other maternal tissues. We did not determine viral biodistribution or measure Lfng in extra-placental organs, so transduction of the maternal liver, kidney, and vasculature cannot be excluded, and the improvements in blood pressure and renal histology may have been mediated wholly or partly outside the placenta. The results therefore establish that systemic Lfng delivery before the insult limits development of the phenotype and maintains placental Notch4 at control levels. They do not establish a placenta-specific mechanism. Distinguishing between these possibilities would require either trophoblast-restricted delivery, for example using a placenta-tropic vector or a trophoblast-specific conditional allele, or a biodistribution study measuring Lfng across maternal organs. We regard this as a necessary step before describing the *in vivo* relationship as placenta-specific.

Conclusions

Within the limitations outlined above, the data support a coherent picture. LFNG is markedly reduced in preeclamptic placenta, its overexpression improves trophoblast proliferation and invasion, and it constrains the induction of NOTCH4 that would otherwise occur in a hypoxia-like state. Whether LFNG has value as a marker of placental dysfunction or as a therapeutic entry point will depend on work that directly connects the enzyme to Notch output by quantifying the cleaved intracellular domain and canonical target genes, and that establishes, through NOTCH4 knockdown and rescue, whether the functional effects of LFNG are mediated through the receptor. Further studies should confirm the reversal under physiological oxygen tension, test intervention after the phenotype is established, determine whether the *in vivo* effect is placenta-specific using trophoblast-restricted delivery, and examine the relationship in models that more closely recapitulate human placentation.

Availability of Data and Materials

The data that support the findings of this study are available from the corresponding author upon reasonable request.

Author Contributions

QP, WJZ and WPZ designed the research study. QP, LLF, CGS and SW performed the research. WJZ, WPZ and YGY analyzed the data. QP drafted the article. All authors contributed to the important editorial changes in the manuscript. All authors read and approved the final manuscript. All authors have participated sufficiently in the work to take public responsibility for appropriate portions of the content and agreed to be accountable for all aspects of the work in ensuring that questions related to its accuracy or integrity.

Ethics Approval and Consent to Participate

The use of human placental tissue was approved by the Medical Ethics Committee of Jiangdu People's Hospital Affiliated to Yangzhou University (approval number YJRY-2022-K-002, granted on 21 January 2022), and all procedures were conducted in accordance with the Declaration of Helsinki. Written informed consent was obtained from all participants. The animal study was approved by The Medical College of Yangzhou University ethics committee (ethics number: YXYLL-2024-094, granted on 26 July 2024). Mice were housed and handled according to institutional guidelines for the care and use of laboratory animals, and the work was reported in accordance with the ARRIVE guidelines 2.0.

Acknowledgment

Not applicable.

Funding

This work was supported by the Suzhou Municipal Health Commission Science and Technology Development Project (Grant No. SLT2023033).

Conflict of Interest

The authors declare no conflict of interest.

Supplementary Material

Supplementary material associated with this article can be found, in the online version, at https://doi.org/10.24976/Discov.Med.202638214.269.

References

[1] Chiang YT, Seow KM, Chen KH. The Pathophysiological, Genetic, and Hormonal Changes in Preeclampsia: A Systematic Review of the Molecular Mechanisms. International Journal of Molecular Sciences. 2024; 25: 4532. https://doi.org/10.3390/ijms25084532

[2] Kovacheva VP, Venkatachalam S, Pfister C, Anwer T. Preeclampsia and eclampsia: Enhanced detection and treatment for morbidity reduction. Best Practice & Research. Clinical Anaesthesiology. 2024; 38: 246–256. https://doi.org/10.1016/j.bpa.2024.11.001

[3] Dimitriadis E, Rolnik DL, Zhou W, Estrada-Gutierrez G, Koga K, Francisco RPV, et al. Pre-eclampsia. Nature Reviews. Disease Primers. 2023; 9: 8. https://doi.org/10.1038/s41572-023-00417-6

[4] Countouris M, Mahmoud Z, Cohen JB, Crousillat D, Hameed AB, Harrington CM, et al. Hypertension in Pregnancy and Postpartum: Current Standards and Opportunities to Improve Care. Circulation. 2025; 151: 490–507. https://doi.org/10.1161/CIRCULATIONAHA.124.073302

[5] Stephansson O, Sandström A. Can short- and long-term maternal and infant risks linked to hypertension and diabetes during

pregnancy be reduced by therapy? Journal of Internal Medicine. 2024; 296: 216–233. https://doi.org/10.1111/joim.13823

[6] Tabacco S, Ambrosii S, Polsinelli V, Fantasia I, D'Alfonso A, Ludovisi M, et al. Pre-Eclampsia: From Etiology and Molecular Mechanisms to Clinical Tools-A Review of the Literature. Current Issues in Molecular Biology. 2023; 45: 6202–6215. https://doi.org/10.3390/cimb45080391

[7] Elovitz MA, Gee EPS, Delaney-Busch N, Moe AB, Reddy M, Khodursky A, et al. Molecular subtyping of hypertensive disorders of pregnancy. Nature Communications. 2025; 16: 2948. https://doi.org/10.1038/s41467-025-58157-y

[8] Kornacki J, Olejniczak O, Sibiak R, Gutaj P, Wender-Ożegowska E. Pathophysiology of Pre-Eclampsia-Two Theories of the Development of the Disease. International Journal of Molecular Sciences. 2023; 25: 307. https://doi.org/10.3390/ijms25010307

[9] Sugulle M, Fiskå BS, Jacobsen DP, Fjeldstad HE, Staff AC. Placental Senescence and the Two-Stage Model of Preeclampsia. American Journal of Reproductive Immunology (New York, N.Y.: 1989). 2024; 92: e13904. https://doi.org/10.1111/aji.13904

[10] Hoffman MK. The great obstetrical syndromes and the placenta. BJOG: an International Journal of Obstetrics and Gynaecology. 2023; 130: 8–15. https://doi.org/10.1111/1471-0528.17613

[11] Varberg KM, Dominguez EM, Koseva B, Varberg JM, McNally RP, Moreno-Irusta A, et al. Extravillous trophoblast cell lineage development is associated with active remodeling of the chromatin landscape. Nature Communications. 2023; 14: 4826. https://doi.org/10.1038/s41467-023-40424-5

[12] Zhang L, Liu J, Feng X, Lash GE. Unraveling the mysteries of spiral artery remodeling. Placenta. 2023; 141: 51–56. https://doi.org/10.1016/j.placenta.2023.05.013

[13] Brouwers L, de Gier S, Vogelvang TE, Veerbeek JHW, Franx A, van Rijn BB, et al. Prevalence of placental bed spiral artery pathology in preeclampsia and fetal growth restriction: A prospective cohort study. Placenta. 2024; 156: 1–9. https://doi.org/10.1016/j.placenta.2024.08.010

[14] Liu CC, Zhang Y, Kim YJ, Hamilton EJ, Xu B, Limas J, et al. β3-adrenergic agonist counters oxidative stress and Na+-K+ pump inhibitory S-glutathionylation of placental cells: implications for preeclampsia. American Journal of Physiology. Cell Physiology. 2025; 328: C27–C39. https://doi.org/10.1152/ajpcell.00379.2024

[15] Huang X, Jia L, Jia Y, Xu X, Wang R, Wei M, et al. sFlt-1-enriched exosomes induced endothelial cell dysfunction and a preeclampsia-like phenotype in mice. Cytokine. 2023; 166: 156190. https://doi.org/10.1016/j.cyto.2023.156190

[16] Dietrich B, Kunihs V, Lackner AI, Meinhardt G, Koo BK, Pollheimer J, et al. NOTCH3 signalling controls human trophoblast stem cell expansion and differentiation. Development (Cambridge, England). 2023; 150: dev202152. https://doi.org/10.1242/dev.202152

[17] Meng Y, Bo Z, Feng X, Yang X, Handford PA. The Notch Signaling Pathway: Mechanistic Insights in Health and Disease. Engineering. 2024; 34: 212–232. https://doi.org/10.1016/j.eng.2023.11.011

[18] Liu L, Tang L, Chen S, Zheng L, Ma X. Decoding the molecular pathways governing trophoblast migration and placental development; a literature review. Frontiers in Endocrinology. 2024; 15: 1486608. https://doi.org/10.3389/fendo.2024.1486608

[19] Qi G, Gong Y, Li Y, Jin Y, Chi S, Zhang W, et al. Insufficient expression of VTN promotes the development of early-onset severe preeclampsia through the HEY1/autophagy signaling pathway. Placenta. 2025; 168: 56–66. https://doi.org/10.1016/j.placenta.2025.06.011

[20] Salvi S, Fruci S, Lacconi V, Totaro Aprile F, Rullo R, Stuhlmann H, et al. Effect of Pravastatin on Placental Expression of Epidermal Growth Factor-like Domain 7 in Early-Onset Pre-Eclampsia: A New Potential Mechanism of Action. Biomedicines. 2024; 12: 1929. https://doi.org/10.3390/biomedicines12081929

[21] Takebe N, Sugita Y, Takada S, Muraki K, Dunwoodie SL, Hojo M, et al. Notch4 is essential for the maintenance of vascular homeostasis in the young adult pituitary posterior lobes. Scientific Reports. 2025; 15: 31153. https://doi.org/10.1038/s41598-025-17225-5

[22] Arutyunyan A, Roberts K, Troulé K, Wong FCK, Sheridan MA, Kats I, et al. Spatial multiomics map of trophoblast development in early pregnancy. Nature. 2023; 616: 143–151. https://doi.org/10.1038/s41586-023-05869-0

[23] Kakuda S, Haltiwanger RS. Deciphering the Fringe-Mediated Notch Code: Identification of Activating and Inhibiting Sites Allowing Discrimination between Ligands. Developmental Cell. 2017; 40: 193–201. https://doi.org/10.1016/j.devcel.2016.12.013

[24] Ramesh PS, Chu LF. Species-specific roles of the Notch ligands, receptors, and targets orchestrating the signaling landscape of the segmentation clock. Frontiers in Cell and Developmental Biology. 2024; 11: 1327227. https://doi.org/10.3389/fcell.2023.1327227

[25] Gong X, Zheng C, Jia H, Liu Y, Yang R, Chen Z, et al. A pan-cancer analysis revealing the role of LFNG, MFNG and RFNG in tumor prognosis and microenvironment. BMC Cancer. 2023; 23: 1065. https://doi.org/10.1186/s12885-023-11545-3

[26] Chung WC, Zhang S, Atfi A, Xu K. Lfng-expressing centroacinar cell is a unique cell-of-origin for p53 deficient pancreatic cancer. Oncogene. 2025; 44: 348–362. https://doi.org/10.1038/s41388-024-03226-7

[27] Li Q, Wei X, Zhang Y, Zeng W, Lin Y. Trophoblast adaptation to hypoxia: balance and dysfunction. Cell Communication and Signaling: CCS. 2025; 23: 538. https://doi.org/10.1186/s12964-025-02531-2

[28] Gu Y, Cooper D, Lewis DF, Zoorob D, Wang Y. Oxidative stress contributes to hypermethylation of Histone H3 lysine 9 in placental trophoblasts from preeclamptic pregnancies. Frontiers in Endocrinology. 2024; 15: 1371220. https://doi.org/10.3389/fendo.2024.1371220

[29] Guo M, Niu Y, Xie M, Liu X, Li X. Notch signaling, hypoxia, and cancer. Frontiers in Oncology. 2023; 13: 1078768. https://doi.org/10.3389/fonc.2023.1078768

[30] Gestational Hypertension and Preeclampsia: ACOG Practice Bulletin, Number 222. Obstetrics and Gynecology. 2020; 135: e237–e260. https://doi.org/10.1097/AOG.0000000000003891

[31] Tveriakhina L, Scanavachi G, Egan ED, Da Cunha Correia RB, Martin AP, Rogers JM, et al. Temporal dynamics and stoichiometry in human Notch signaling from Notch synaptic complex formation to nuclear entry of the Notch intracellular domain. Developmental Cell. 2024; 59: 1425–1438.e8. https://doi.org/10.1016/j.devcel.2024.03.021

[32] Lamar E, Deblandre G, Wettstein D, Gawantka V, Pollet N, Niehrs C, et al. Nrarp is a novel intracellular component of the Notch signaling pathway. Genes & Development. 2001; 15: 1885–1899. https://doi.org/10.1101/gad.908101

[33] Gustafsson MV, Zheng X, Pereira T, Gradin K, Jin S, Lundkvist J, et al. Hypoxia requires notch signaling to maintain the undifferentiated cell state. Developmental Cell. 2005; 9: 617–628. https://doi.org/10.1016/j.devcel.2005.09.010

[34] Tamamura Y, Terai K, Yamaguchi A. Notch signaling modulates Fgf23 expression through crosstalk with hypoxia and PTH pathways in osteogenic cells. Molecular and Cellular Endocrinology. 2025; 610: 112663. https://doi.org/10.1016/j.mce.2025.112663

[35] de Alwis N, Binder NK, Beard S, Mangwiro YT, Kadife E,

Cuffe JS, et al. The L-NAME mouse model of preeclampsia and impact to long-term maternal cardiovascular health. Life Science Alliance. 2022; 5: e202201517. https://doi.org/10.26508/lsa.202201517

[36] Barton A, Jaśkiewicz M, Więch-Walów A, Moszyńska A, Cabaj A, Wielockx B, et al. Challenges in mimicking hypoxia: insights into HIF-regulated MiRNA expression induced by DMOG and CoCl2. Cell Communication and Signaling: CCS. 2025; 23: 454. https://doi.org/10.1186/s12964-025-02459-7

[37] Lamela F, Bologna-Molina R, Parietti F, Pereira-Prado V, Millán M, Silva A, et al. Differential effects of coverslip-induced hypoxia and cobalt chloride mimetic hypoxia on cellular stress, metabolism, and nuclear structure. Tissue & Cell. 2024; 88: 102408. https://doi.org/10.1016/j.tice.2024.102408

[38] Abou-Kheir W, Barrak J, Hadadeh O, Daoud G. HTR-8/SVneo cell line contains a mixed population of cells. Placenta. 2017; 50: 1–7. https://doi.org/10.1016/j.placenta.2016.12.007